Pancreatic liposarcoma: A case report

YAN ZHAO[1], SHIKANG HU[2], HUAJUN SUN[3], JIYUN YANG[4] and TAO LU[1]

[1]Department of Radiology, Sichuan Provincial People's Hospital, University of Electronic Science and Technology of China, Chengdu, Sichuan 610072, P.R. China; [2]Department of Radiology, School of Medicine, University of Electronic Science and Technology of China, Chengdu, Sichuan 610054, P.R. China; [3]Department of Pathology, Sichuan Provincial People's Hospital, University of Electronic Science and Technology of China, Chengdu, Sichuan 610072, P.R. China; [4]Sichuan Provincial Key Laboratory for Human Disease Gene Study, Center of Medical Genetics, Sichuan Academy of Medical Sciences and Sichuan Provincial People's Hospital, University of Electronic Science and Technology of China, Chengdu, Sichuan 610072, P.R. China

Received August 16, 2024; Accepted February 5, 2025

DOI: 10.3892/ol.2025.15014

Abstract. Primary liposarcoma (LPS) of the pancreas is extremely rare. The present report describes an additional case of primary pancreatic LPS and reviews the current literature. A 40-year-old female patient that initially presented with a fever was subsequently found to have a pancreatic tumor. CT was used to identify a heterogeneous mass in the pancreatic head and body, which had a notable absence of fat components. The tumor exhibited slightly heterogeneous enhancement during the arterial phase, moderate enhancement in the venous phase and persistent enhancement in the delayed phase, with encapsulation of the common hepatic artery, splenic vein and portal vein. The patient underwent a successful distal pancreatectomy and splenectomy. Pathological examination and next-generation sequencing confirmed the diagnosis of dedifferentiated LPS (DDLPS). The present report elucidated the CT findings of this rare case of DDLPS of the pancreas, characterized by vascular invasion and progressive enhancement but without fat components, which can serve as a reference for the diagnosis of this uncommon tumor. The uncommon CT manifestation makes differentiation from pancreatic neuroendocrine tumors particularly challenging based on imaging characteristics.

Correspondence to: Dr Tao Lu, Department of Radiology, Sichuan Provincial People's Hospital, University of Electronic Science and Technology of China, 32 West Second Section, First Ring Road, Chengdu, Sichuan 610072, P.R. China
E-mail: 345248302@qq.com

Abbreviations: STS, soft tissue sarcoma; LPS, liposarcoma; DDLPS, dedifferentiated LPS; WDLPS, well-differentiated LPS; MLPS, myxoid/round cell LPS; PLPS, pleomorphic LPS; MDM2, murine double minute 2; NGS, next-generation sequencing; pNET, pancreatic neuroendocrine tumor; F-pNET, functional pNET; NF-pNET, non-functional pNET

Key words: pancreatic LPS, DDLPS, CT

Introduction

Soft tissue sarcoma (STS) is a category of rare malignant tumors that can arise in various locations within the body, with ~50% occurring in the extremities, 40% in the trunk and retroperitoneum, and 10% in the head and neck (1). Its incidence is <6 cases per 100,000 individuals, which represents 1-2% of all adult cancers (2). The etiology of the majority of STS is unknown; however, in most cases, the risk of developing sporadic STS is increased in patients with a history of previous radiotherapy and certain genetic mutations (1). Surgery is a mainstay of sarcoma treatment, and radiation is used for unresectable tumors and as a neoadjuvant or an adjuvant to resection (3). Common soft-tissue sarcomas include malignant fibrous histiocytoma, liposarcoma (LPS), leiomyosarcoma and synovial sarcoma (4). LPS, a malignant neoplasm differentiated by adipocytes, represents one of the most prevalent subtypes of STS, accounting for 15-20% of all STS cases (5). According to the characteristics of tumor cells, LPS can be classified into four types: i) Atypical lipomatous/well-differentiated LPS (WDLPS); ii) dedifferentiated LPS (DDLPS); iii) myxoid/round cell LPS (MLPS); and iv) pleomorphic LPS (PLPS) (6).

WDLPS and DDLPS constitute the largest subgroup of LPS, with WDLPS accounting for 40-45% of cases (7). Notedly, up to 10% of WDLPS cases may be dedifferentiated to DDLPS (7). DDLPS is characterized by the presence of both WDLPS components and non-lipogenic components (8). WDLPS and DDLPS share common genetic aberrations involving high-level amplifications of murine double minute 2 (MDM2) and CDK4 in the chromosomal region 12q14-15 (7). Immunohistochemistry analysis frequently demonstrates positive expression of MDM2 and CDK4, which may be accompanied by p16 positivity (9).

The most frequent site of DDLPS is the retroperitoneum. Primary LPS of the pancreas remains exceptionally rare (10). Only 9 cases have been reported in the English literature since 1979, Among these cases, 4 were classified as DDLPS (10-13), 3 as WDLPS (14-16), 1 as MLPS (17) and 1 as PLPS (18). Additionally, only 1 case (13) of pancreatic DDLPS lacking a fat component has been reported. The present study reports

another case of primary pancreatic DDLPS without fat components, with CT features described in detail.

Case report

In May 2023, a 40-year-old female patient presented with a fever that had persisted for several days without accompanying symptoms to Sichuan Provincial People's Hospital (Chengdu, China) for treatment. The medical and family history of the patient were unremarkable, and the patient was in normal physical condition. All laboratory data, including tumor markers such as carcinoembryonic antigen (<1.73 ng/ml; normal range, ≤5 ng/ml) and carbohydrate antigen 19-9 (10.97 U/ml; normal range, ≤43 U/ml) were within normal limits. Abdominal CT (Fig. 1A) demonstrated a solid mass measuring 2.4x4.5 cm located in the pancreatic head and body. The tumor was heterogeneous and lacked a fat component. Dynamic contrast-enhanced CT demonstrated slightly heterogeneous enhancement in the arterial phase (Fig. 1B), moderate enhancement in the venous phase (Fig. 1D) and persistent enhancement in the delayed phase (Fig. 1E), with encapsulation of the common hepatic artery, splenic vein and portal vein (Fig. 1C and F). No lymphadenopathy was observed.

The patient underwent distal pancreatectomy and splenectomy in May 2023. Laparotomy determined that the tumor measured 4x4x3 cm in the head and body of the pancreas. The tumor firmly adhered to the splenic vein, inferior mesenteric vein and common hepatic artery, and showed invasion into the duodenum. Grossly, the tumor was elastic and firm, centered with fish flesh-like texture. Histologically, the tumor predominantly consisted of medium and highly atypical spindle cells alongside multivacuolated lipoblasts (Fig. 2A). H&E staining was performed as follows: The tumor tissues were fixed in 10% formalin for >24 h at 25˚C (Beijing BioDee Biotechnology Co., Ltd.), followed by gradient alcohol dehydration and embedding in paraffin. Subsequently, 3-μm thick sections were sectioned and stained with H&E. Sections were stained with hematoxylin for 5 min at room temperature, rinsed with running water for 3 min, incubated with 1% HCl/ethyl for 3 sec, rinsed with running water for 1 sec, stained with bluing solution for 10 sec at room temperature, rinsed with running water for 5 sec, stained with eosin Y stain (water soluble; 0.5%) for 3 min at room temperature, incubated with 95% ethyl alcohol for 2 sec, incubated with 100% ethyl alcohol for 2 sec twice and incubated with 100% xylene three times, followed by neutral balsam mounting. The images were acquired using an Olympus BX53 light microscope (Olympus Corporation).

Immunohistochemistry analysis of the tissue sample revealed positive expression of CD34 (Fig. 2B), CDK4 (Fig. 2C), MDM2 (Fig. 2D), catenin (Fig. 2E), desmin (Fig. 2F) and p16 (Fig. 2G), and negative expression of S-100 (Fig. 2H), CD68 (Fig. 2I), creatine kinase (Fig. 2J), epithelial membrane antigen (Fig. 2K), HMB-45 (Fig. 2L), smooth muscle actin (Fig. 2M), STAT6 (Fig. 2N) and mucin 4 (Fig. 2O). The Ki-67 (Fig. 2P) index was 20%. IHC staining was conducted according to the manufacturer's protocol (KIT-9701/9706; Fuzhou Maixin Biotechnology Development Co., Ltd.). H&E staining was performed as follows: The tumor tissues were fixed in 10% formalin for >24 h at 25˚C (Beijing BioDee Biotechnology Co., Ltd.), followed by gradient alcohol dehydration and embedding in paraffin. Subsequently, 3-μm thick sections were sectioned and stained with IHC. Tissue sections were dewaxed in xylene and rehydrated in graded alcohols (descending series). Endogenous peroxidase activity was blocked with methanol + 0.3% peroxide (SP KIT-A1) for 10 min at room temperature. Tissue sections were pretreated with heat-induced antigen retrieval using citrate buffer (pH 6.0; MVS-0100) for 10 min at 98˚C. Non-immune serum of animals (SP KIT-B1; 10% goat serum; Fuzhou Maixin Biotechnology Development Co., Ltd.) was applied for protein blocking at room temperature for 20 min prior to incubation with the first primary antibody. Sections were incubated with a primary antibody overnight at 4˚C, incubated with 3% H_2O_2 for 10 min, incubated with 10% goat serum (Fuzhou Maixin Biotechnology Development Co., Ltd.) at room temperature for 20 min and finally incubated with primary antibody at 4˚C overnight. The primary antibodies included CD34 (1:100; Kit-0004; Fuzhou Maixin Biotechnology Development Co., Ltd.), CDK4 (1:100; RMA-0771; Fuzhou Maixin Biotechnology Development Co., Ltd.), catenin (1:100; RMA-1054; Fuzhou Maixin Biotechnology Development Co., Ltd.), desmin (1:100; MAB-0766; Fuzhou Maixin Biotechnology Development Co., Ltd.), Ki-67 (1:100; RMA-0542; Fuzhou Maixin Biotechnology Development Co., Ltd.), MDM2 (1:100; MAB-0774; Fuzhou Maixin Biotechnology Development Co., Ltd.), p16 (1:100; MAB-0673; Fuzhou Maixin Biotechnology Development Co., Ltd.), CD68 (1:100; MAB-0687; Fuzhou Maixin Biotechnology Development Co., Ltd.), EMA (1:100; Kit-0011; Fuzhou Maixin Biotechnology Development Co., Ltd.), HMB-45 (1:100; MAB-0098; Fuzhou Maixin Biotechnology Development Co., Ltd.), SMA (1:100; MAB-0890; Fuzhou Maixin Biotechnology Development Co., Ltd.), STAT6 (1:100; RMA-0845; Fuzhou Maixin Biotechnology Development Co., Ltd.), mucin 4 (1:100; MAB-0749; Fuzhou Maixin Biotechnology Development Co., Ltd.), Ki-67 (1:100; MAB-0672; Fuzhou Maixin Biotechnology Development Co., Ltd.), CK (1:100; Kit-0004; Fuzhou Maixin Biotechnology Development Co., Ltd.) and s-100 (1:100; Kit-0007; Fuzhou Maixin Biotechnology Development Co., Ltd.) antibodies. Subsequently, the slides were incubated with secondary antibodies (1:100; KIT-9701/9706; Fuzhou Maixin Biotechnology Development Co., Ltd.; peroxidase/DAB+) for 10 min at room temperature, and then stained with DAB and hematoxylin for 1 min at 25˚C. Finally, images were captured using a laboratory microscopy (Olympus BX53 light microscope; Olympus Corporation), and the integrated optical density of the immunohistochemistry-positive areas was analyzed using Image-Pro Plus 6.0 software (Media Cybernetics, Inc.).

Next-generation sequencing (NGS) demonstrated amplifications of the CDK4 and MDM2 genes. Briefly, genomic DNA was extracted from formalin-fixed paraffin-embedded sections using the QIAamp DNA FFPE Tissue Kit (cat. no. 56404; Qiagen GmbH), and quantified using a Qubit® 3.0 Fluorometer (Invitrogen; Thermo Fisher Scientific, Inc.) using the dsDNA HS Assay Kit (cat. no. Q32854; Thermo Fisher Scientific, Inc.). Libraries were prepared using 2,420 ng genomic DNA using a Geneseeq Prime 425-gene panel (cat. no. 20233401452; Nanjing Geneseeq Technology, Inc.) according to the manufacturer's protocol. Libraries were quantified by quantitative polymerase chain reaction (qPCR) using Illumina p5 (5'-AAT

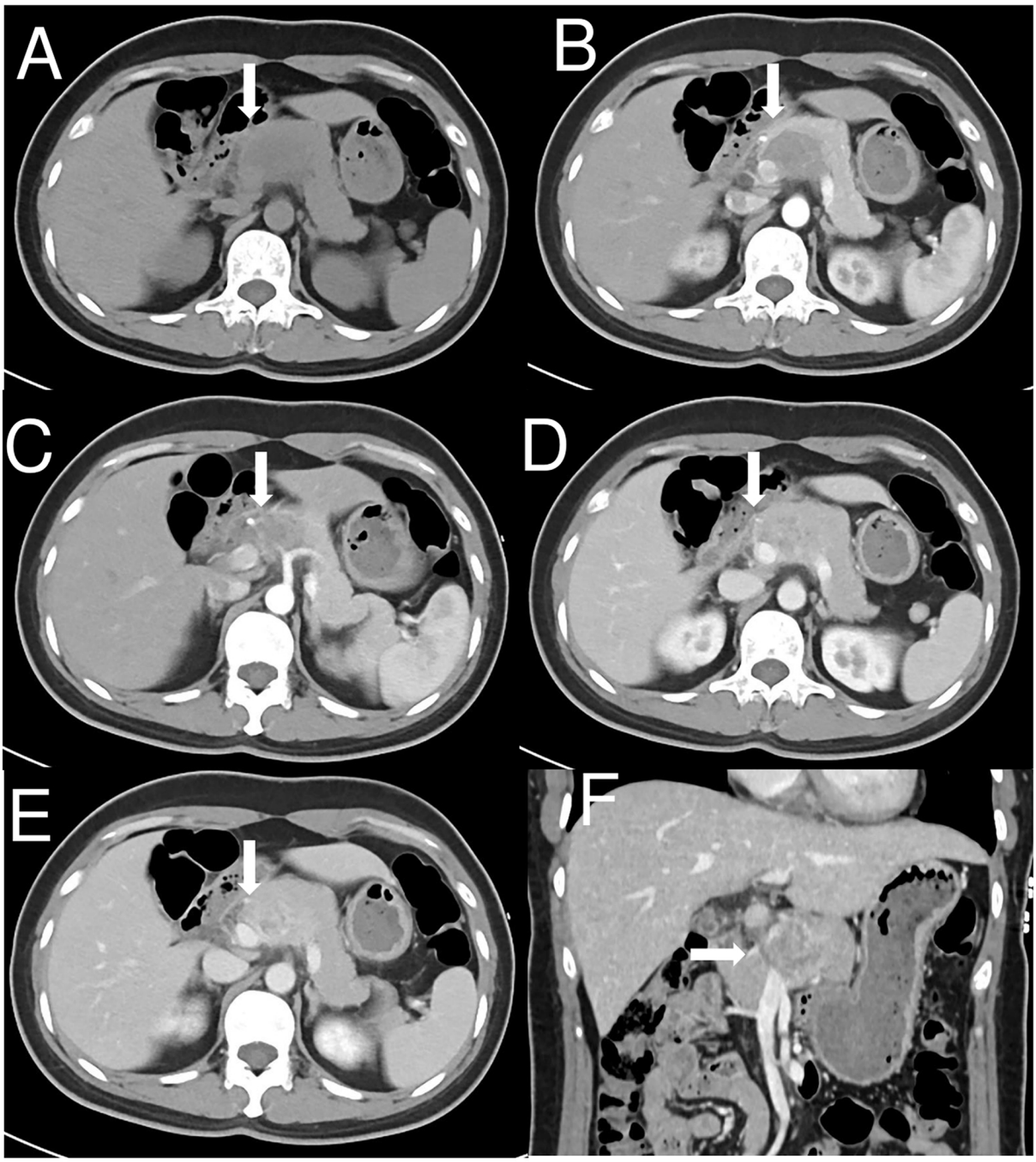

Figure 1. Radiological findings. (A) Unenhanced axial CT image revealing a heterogenous mass in the pancreatic head and body (arrow). (B) Arterial phase axial CT image showing slight enhancement of the lesion (arrow). (C) Arterial phase axial CT image showing the tumor invaded the common hepatic artery(arrow). (D) Venous phase axial CT image indicating further uneven enhancement of the lesion with invasion to the splenic vein (arrow). (E) Delayed phase axial CT image showing persistent enhancement of the lesion (arrow). (F) Delayed phase coronal CT image showing heterogenous enhancement of the lesion with invasion to the portal vein (arrow).

GATACGGCGACCACCGA-3') and p7 (5'-CAAGCAGAA GACGGCATACGAGAT-3') primers in the KAPA Library Quantification kit (cat. no. KK4824; Kapa Biosystems; Roche Diagnostics). qPCR was run using the KAPA Library Quantification kit on the QuantStudio™ 5 Real-Time PCR System (Thermo Fisher Scientific, Inc.). qPCR cycling conditions were as follows: Initial denaturation at 95˚C for 5 min, followed by 35 cycles of denaturation at 95˚C for 30 sec and annealing/extension/data acquisition at 60˚C for 30 sec. The standard curve was generated using QuantStudio 5 Real-Time PCR System v1.6.0 software (Thermo Fisher Scientific, Inc.). The standard curve was used to calculate the concentration of the library according to the manufacturer's protocol for the KAPA Library Quantification kit. The library fragment size was determined using a Bioanalyzer 2100 (Agilent Technologies, Inc.). Different libraries with unique indices were pooled together in desirable ratios for up to 4,030 pmol/μl of total library input. The library sequencing (loading concentration of the final library, 100-200 pM) was performed on Illumina NovaSeq platforms (Illumina, Inc.) using 150-bp paired-end

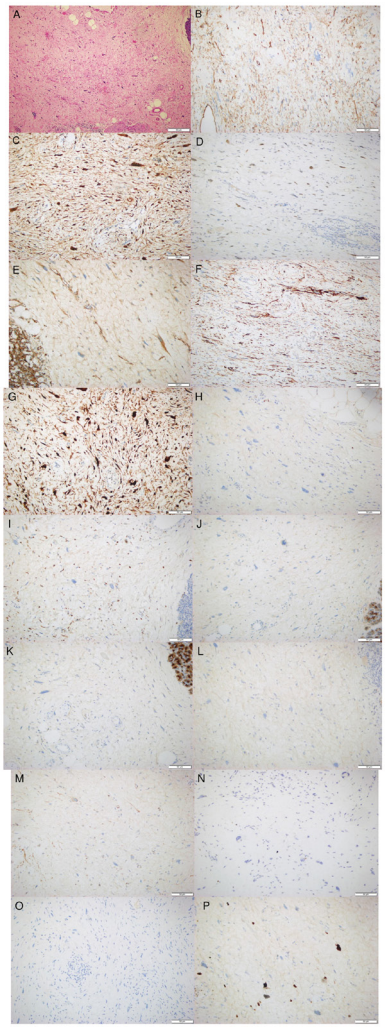

Figure 2. Representative images of pathological findings. (A) H&E staining of the specimen demonstrated that the tumor cells predominantly consisted of medium and highly atypical spindle cells with the presence of multivacuolated lipoblasts (scale bar, 50 μm). Positive nuclear immunostaining in neoplastic cells of (B) CD34, (C) CDK4, (D) murine double minute 2, (E) catenin, (F) desmin and (G) P16 (scale bar, 50 μm). (H) S-100, (I) CD68, (J) creatine kinase, (K) epithelial membrane antigen, (L) HMB-45, (M) smooth muscle actin, (N) STAT6 and (O) mucin 4 negative nuclear immunostaining in neoplastic cells (scale bar, 50 μm). (P) The positive index of Ki-67 in tumor cells was ~20% (scale bar, 50 μm).

sequencing. The average coverage depth was 1,939.24X. For mutation calling, Trimmomatic (version 0.38; http://www.usadellab.org/cms/index.php?page=trimmomatic) was used for FASTQ file quality control. Qualified reads were then mapped to the reference human genome (hg19) using Burrows-Wheeler Aligner (version 0.7.17.tar.bz2; http://bio-bwa.sourceforge.net/). Somatic mutations were detected using VarScan2 (version 2.4.4, http://dkoboldt.github.io/varscan) with default parameters. Annotation was performed using ANNOVAR (version 2019-10-24 00:05:27-0400; https://annovar.openbioinformatics.org/) using the reference human genome (GRCh37/hg19). Finally, the tumor was diagnosed as DDLPS based on histological, immunohistochemical and NGS tests. The postoperative recovery was uneventful, and the patient was under surveillance without additional treatment. The abdominal ultrasound exhibited no signs of recurrence during the follow-up between May 2023 and June 2024.

Discussion

LPS is the most common type of STS and typically occurs in the extremities or retroperitoneum (10). The occurrence of LPS in visceral organs, such as the pancreas, is extremely rare, with only individual cases reported, which leads to the uncertainty regarding the exact incidence. The peak incidence of pancreatic LPS occurs in the sixth and seventh decades of life without obvious sex predilection (10). In the reported cases thus far, including the present study, the patients included 7 female and 3 male patients, indicating a slight female predominance (Table I). Patient age ranged between 24 and 81 years, with a mean age of 51.6 years. This in contrast to retroperitoneum LPS, where patients are generally older without a noted sex preference (19).

Clinical presentations of pancreatic LPS can be asymptomatic or nonspecific, including abdominal pain, distension and diarrhea (13). In the present case, the patient attended a hospital because of a fever. The pancreatic tumor was identified incidentally, without gastrointestinal symptoms. The literature indicates that the average tumor diameter is 17.5 cm in symptomatic patients and 5.2 cm in asymptomatic patients. Symptomatic patients tend to have larger tumors (10-18). The tumor reported in the present case measured 4 cm, which was in accordance with the absence of symptoms due to tumor compression.

Pancreatic LPS has been identified in the pancreatic head and neck in 1 case, pancreatic body in 2 cases, pancreatic body and tail in 2 cases and pancreatic tail in 4 cases (Table II). In the present study, the tumor was situated in the head and body of the pancreas, which was relatively rare. In half of the reported 10 cases of pancreatic LPS, the tumor margins were unclear. As the tumor grows, it can invade surrounding organs, including the duodenum, spleen and left adrenal gland (10-18).

DDLPS is a malignant adipocytic neoplasm defined as the transition from WDLPS to a non-lipogenic sarcoma with morphologically distinct components, a mature adipocytic component (atypical lipomatous tumor; WDLPS) and a higher-grade non-lipogenic (dedifferentiated) component (8). Histologically, DDLPS typically manifests as undifferentiated pleomorphic or spindle cell sarcomas, usually displaying moderate or high cellularity with moderate to significant pleomorphism (7).

Both WDLPS and DDLPS exhibit a simple genomic profile characterized by the amplification of the 12q14-15 region, while the increased expression of MDM2 and CDK4 is consistent with this amplification (7,20). Immunohistochemical analyses of a range of sarcomas have shown sensitivities of 95% for MDM2 and 92% for CDK4, with specificities of 81 and 95%, respectively (21). According to the relevant literature, the combination of p16 with MDM2 and CDK4 is insufficient to fully meet the needs of distinguishing between WDLPS and DDLPS occasionally, with 100% of WDLPS and 93% of DDLPS expressing at least two of the three markers, and 68% of WDLPS and 72% of DDLPS expressing all three markers (9,22). LPS harbors characteristic genetic abnormalities, including amplification of the MDM2 and CDK4 region (7). Consequently, molecular genetics and cytogenetic analyses (such as NGS) can serve as valuable ancillary diagnostic tools when significant histological features are absent (23).

Table I. Clinical characteristics of patients with pancreatic LPS.

First author/s, year	Age, years	Sex	Symptoms	Surgery	LPS subtype	Immunohistochemistry	Outcome (follow-up duration)	(Refs.)
Tanabe *et al*, 2022	81	F	None	DPS	DDLPS	CDK4(+) and MDM2(-)	Recurrence (7 months)	(10)
Cao *et al*, 2019	72	F	None	DPSA	WDLPS	N/A	N/A	(16)
Liu *et al*, 2019	28	F	Abdominal pain	DPS	DDLPS	MDM2(+)	No recurrence (26 months)	(11)
Han *et al*, 2017	29	F	Abdominal pain	DPS	DDLPS	MDM2(-)	Recurrence (1 year)	(12)
Machado *et al*, 2016	42	M	Abdominal pain	DPS	DDLPS with high grade components	MDM2(+)	No recurrence (5 years)	(13)
Matthews *et al*, 2016	65	F	None	DP	WDLPS	MDM2(+)	N/A	(14)
Kuramoto *et al*, 2013	24	M	Abdominal distension	CP	Myxoid	N/A	Recurrence (44 months)	(17)
Dodo, 2005	76	M	Abdominal pain	DPS	WDLPS with area of DDLPS	N/A	No recurrence (26 months)	(15)
Elliott *et al*, 1980	59	F	Abdominal distension	DPS	Pleomorphic	N/A	No recurrence (6 years)	(18)
Present study	40	F	Fever	DPS	DDLPS	CDK4(+) and MDM2(+)	No recurrence (12 months)	-

F, female; M, male; DP, distal pancreatectomy; CP, central pancreatectomy; DPS, distal pancreatectomy and splenectomy; DPSA, DPS and adrenalectomy; N/A, not available; LPS, liposarcoma; DDLPS, dedifferentiated LPS; WDLPS, well-differentiated LPS; MDM2, murine double minute 2.

Table II. Imaging features of patients with pancreatic liposarcoma.

First author/s, year	Location	Size, cm	Vascular invasion	Abdominal lymphadenopathy	Fat component	Imaging modality	Precontrast	Arterial phase	Venous phase	Delayed phase	(Refs.)
Tanabe *et al*, 2022	Tail	2.6	N/A	No	Yes	CT/^{18}F-FDG PET	Heterogeneous	Early enhancement	N/A	Delayed enhancement	(10)
Cao *et al*, 2019	Body and tail	9.7	N/A	N/A	Yes	CT	Heterogeneous	N/A	N/A	N/A	(16)
Liu *et al*, 2019	Tail	18.0	No	Yes	N/A	CT	Heterogenous	N/A	N/A	N/A	(11)
Han *et al*, 2017	Tail	20.0	N/A	N/A	N/A	CT	Heterogenous	N/A	N/A	N/A	(12)
Machado *et al*, 2016	Head and neck	6.8	N/A	No	No	MRI	Heterogenous	N/A	N/A	N/A	(13)
Matthews *et al*, 2016	Tail	4.0	N/A	N/A	N/A	CT/PET	Hypointensity	N/A	N/A	N/A	(14)
Kuramoto *et al*, 2013	Body	25.0	N/A	N/A	Yes	CT	Heterogenous	N/A	N/A	N/A	(17)
Dodo, 2005	Body and tail	9.0	N/A	N/A	Yes	CT	Heterogenous	N/A	N/A	N/A	(15)
Elliott *et al*, 1980	Body	16.0	N/A	N/A	N/A	N/A	N/A	N/A	N/A	N/A	(18)
Present study	Head and body	4.0	Yes	No	No	CT	Heterogenous	Slight heterogenous	Moderate heterogenous	Persistent enhancement	-

^{18}F-FDG, 18F-fluorodeoxyglucose; PET, position emission tomography; N/A, not available.

In the present study, H&E staining demonstrated that the tumor cells predominantly consisted of medium and highly atypical spindle cells alongside multivacuolated lipoblasts. Immunohistochemistry showed positive results for MDM2, CDK4 and p16. NGS confirmed amplifications of MDM2 and CDK4. Thus, the final pathology-based diagnosis was established to be DDLPS (24,25).

Besides the present study, seven reports described the CT findings of pancreatic LPS, and one report detailed the MRI findings (Table II). CT showed the tumor was heterogeneous, with low-density areas indicating a fat component in 4 cases (10,15-17). Notably, only one report demonstrated a case of pancreatic DDLPS without fat components (13). A previous report described the MRI finding of a heterogeneous mass with a thick wall and septations (13). To the best of our knowledge, the present report describes the second instance of pancreatic LPS devoid of fat and is the second to illustrate its CT enhancement pattern, characterized by slightly heterogeneous enhancement in the arterial phase, moderate enhancement in the venous phase and persistent enhancement in the delayed phase. The deficiency of fat in this tumor may be attributed to the pathological features of DDLPS, which often predominantly contains non-lipogenic components, complicating the diagnostic process (8). It has been reported that the early enhancement in the arterial phase on CT may reflect vascular growth and the delayed enhancement denotes fibrous components within the tumor (26). Although 2 cases of LPS were located in the pancreatic head, dilation of bile and pancreatic ducts was absent, likely because the tumor did not originate from the epithelial cells of pancreatic ducts (27). To the best of our knowledge, the present study is the first to demonstrate vascular invasion involving the common hepatic artery, splenic vein and portal vein via CT, underscoring the high malignancy of this tumor. Therefore, CT served a pivotal role in characterizing the tumor and its surrounding structures.

Pancreatic LPS needs to be differentiated from several other pancreatic lesions, including solid pseudopapillary tumor, neuroendocrine tumor and pancreatic ductal adenocarcinoma. Solid pseudopapillary tumors usually occur in women aged 20-30 years (28). Typically, these tumors present as encapsulated solid masses with well-defined borders and varying degrees of internal cystic and hemorrhagic degeneration on CT (29). Contrast-enhanced CT images demonstrate progressive delayed enhancement for the solid component, and no enhancement for cystic portions of tumors, but the cyst walls enhance similarly to solid components (29). However, in the present study, the patient was a middle-aged woman, and the tumor was solid without hemorrhage or cystic changes, distinguishing it from solid pseudopapillary tumors.

Pancreatic neuroendocrine tumors (pNETs) can be classified as functional pNETs (F-pNETs) or non-functional pNETs (NF-pNETs) (30). A large proportion of F-pNETs are characterized by well-circumscribed hypervascular lesions, and are typically hyper-enhanced in the arterial phase and wash out in the delayed venous phase (31). Additionally, F-pNETs often present with specific clinical syndromes; insulinomas typically manifest as Whipple's triad (hypoglycemic syndromes, low plasma glucose measured at the time of the symptoms and signs, and relief of symptoms and signs when the glucose is raised to normal) and gastrinoma leading to Zollinger-Ellison syndrome (abdominal pain, gastroesophageal reflux, diarrhea and duodenal ulcers) (32). These clinical syndromes can aid the differentiation of DDLPS from F-PNETs. By contrast, NF-pNETs generally remain asymptomatic before significant tumor compression. Then, NF-pNETs may present with nonspecific abdominal pain, early satiety or weight loss (32). NF-pNETs are usually larger with less intense but more heterogeneous enhancement (31). However, these manifestations are not specific. The present study described a heterogeneous tumor with progressive enhancement, which was challenging to differentiate from NF-pNETs.

Pancreatic ductal adenocarcinoma is typically viewed as a hypo-enhancing mass and the auxiliary signs include dilatation of the biliary and pancreatic duct (double-duct sign), peripancreatic vascular invasion and upstream parenchymal atrophy (33). In the present study, the contrast-enhanced CT showed progressive enhancement of the tumor without dilation of biliary and pancreatic ducts or distal parenchymal atrophy, further differentiating it from pancreatic ductal adenocarcinoma.

Surgery is the gold standard for treatment of LPS (12). All 10 patients reported in the literature underwent surgical intervention, with the specific surgical approach tailored to the tumor location. A key factor influencing prognosis is the adequacy of surgical resection at the time of primary presentation. Although chemotherapy is generally considered to be resisted by WDLPS and DDLPS, it still serves an essential role in treatment (34). First-line therapies for advanced or unresectable DDLPS may include single-agent anthracycline or anthracycline combined with ifosfamide (35). Among the 10 patients, 3 (10,12,17) experienced recurrence post-surgery, although 1 (12) had already received chemotherapy. Regarding the present case, aggressive surgical resection was considered to offer the best chance of cure. The patient showed no recurrence post-surgery with no signs of relapse during the 12-month follow-up.

Regular follow-up is recommended for patients who have undergone complete excision of pancreatic LPS, as local recurrence of LPSs in other organs is common (34). According to previous studies, the local recurrence rate of DDLPS is ~40%, with a metastatic rate of 15-30% (7) and the 5-year survival rate is 49.4% (36).

The rarity of the present case lies in the identification of pancreatic LPS without fat components. Furthermore, the present study demonstrated the enhancement pattern of this fat-deficient pancreatic LPS, which can serve as a reference for the diagnosis of this uncommon tumor. However, a limitation of the present study is the absence of an MRI examination, which typically provides a clearer visualization of lipomatous components. When lipomatous components are diminished in DDLPS, MRI is superior to CT in detecting any residual fat within the tumor (1,13).

In conclusion, pancreatic LPS is extremely rare. It possesses a wide range of onset ages and a female predilection. Imaging is pivotal in detecting and characterizing the tumor and its surrounding structures. Pancreatic LPS may lack fat components and exhibit progressive enhancement, which complicates the differentiation from non-functional neuroendocrine tumors from imaging. The tumor can invade adjacent vascular structures, including the common hepatic

artery, splenic vein and portal vein, but excluding the bile and pancreatic ducts, likely because the tumor did not originate from the epithelial cells of pancreatic ducts. In brief, as both the clinical and imaging manifestations of pancreatic liposarcoma are nonspecific, it is difficult to make a definite diagnosis when fat components are lacking, and final diagnosis hinges upon histological, immunohistochemistry and NGS tests.

Acknowledgements

Not applicable.

Funding

No funding was received.

Availability of data and materials

The data generated in the present study are not publicly available due to the PACS system regulated by Sichuan Provincial People's Hospital but may be requested from the corresponding author.

Authors' contributions

TL conceived and designed the study, and contributed to manuscript drafting. YZ and SH obtained medical images and confirmed the authenticity of all the raw data. JY carried out the high-throughput sequencing experiments and performed the bioinformatics analysis. HS performed the histological examination of the tumor, and contributed to writing the manuscript. All authors have read and approved the final version of the manuscript.

Ethics approval and consent to participate

The present study protocol was approved by the Institutional Review Board of the Department of Radiology, Sichuan Provincial People's Hospital, and the University of Electronic Science and Technology of China (approval no. 2024-709; Chengdu, China).

Patient consent for publication

Written and verbal consent was obtained from the patient for publication.

Competing interests

The authors declare that they have no competing interests.

References

1. Ardakani AHG, Woollard A, Ware H and Gikas P: Soft tissue sarcoma: Recognizing a rare disease. Cleve Clin J Med 89: 73-80, 2022.
2. Bourcier K, Le Cesne A, Tselikas L, Adam J, Mir O, Honore C and de Baere T: Basic knowledge in soft tissue sarcoma. Cardiovasc Intervent Radiol 42: 1255-1261, 2019.
3. Gamboa AC, Gronchi A and Cardona K: Soft-tissue sarcoma in adults: An update on the current state of histiotype-specific management in an era of personalized medicine. CA Cancer J Clin 70: 200-229, 2020.
4. Gilbert NF, Cannon CP, Lin PP and Lewis VO: Soft-tissue sarcoma. J Am Acad Orthop Surg 17: 40-47, 2009.
5. Lee ATJ, Thway K, Huang PH and Jones RL: Clinical and molecular spectrum of liposarcoma. J Clin Oncol 36: 151-159, 2018.
6. Sbaraglia M, Bellan E and Dei Tos AP: The 2020 WHO classification of soft tissue tumours: News and perspectives. Pathologica 113: 70-84, 2020.
7. Thway K: Well-differentiated liposarcoma and dedifferentiated liposarcoma: An updated review. Semin Diagn Pathol 36: 112-121, 2019.
8. Dehner CA, Hagemann IS and Chrisinger JSA: Retroperitoneal dedifferentiated liposarcoma. Am J Clin Pathol 156: 920-925, 2021.
9. Kammerer-Jacquet SF, Thierry S, Cabillic F, Lannes M, Burtin F, Henno S, Dugay F, Bouzillé G, Rioux-Leclercq N, Belaud-Rotureau MA and Stock N: Differential diagnosis of atypical lipomatous tumor/well-differentiated liposarcoma and dedifferentiated liposarcoma: Utility of p16 in combination with MDM2 and CDK4 immunohistochemistry. Hum Pathol 59: 34-40, 2017.
10. Tanabe M, Matsui H, Higashi M, Tokumitsu Y, Nagano H and Ito K: Pancreatic liposarcoma: A case report. Abdom Radiol (NY) 47: 1912-1916, 2022.
11. Liu Z, Fan WF, Li GC, Long J, Xu YH and Ma G: Huge primary dedifferentiated pancreatic liposarcoma mimicking carcinosarcoma in a young female: A case report. World J Clin Cases 7: 1344-1350, 2019.
12. Han T, Luan Y, Xu Y, Yang X, Li J, Liu R, Li Q and Zheng Z: Successful treatment of advanced pancreatic liposarcoma with apatinib: A case report and literature review. Cancer Biol Ther 18: 635-639, 2017.
13. Machado MCC, Fonseca GM, de Meirelles LR, Zacchi FFS and Bezerra ROF: Primary liposarcoma of the pancreas: A review illustrated by findings from a recent case. Pancreatology 16: 715-718, 2016.
14. Matthews M, Nelson S, Hari D and French S: Well differentiated liposarcoma, sclerosing type, of the pancreas a case report. Exp Mol Pathol 101: 320-322, 2016.
15. Dodo IM, Adamthwaite JA, Jain P, Roy A, Guillou PJ and Menon KV: Successful outcome following resection of a pancreatic liposarcoma with solitary metastasis. World J Gastroenterol 11: 7684-7685, 2005.
16. Cao D, Wang J and Guo L: Pancreatic liposarcoma: A rare cause of pancreatic mass in adult. J Gastroenterol Hepatol 34: 1275, 2019.
17. Kuramoto K, Hashimoto D, Abe S, Chikamoto A, Beppu T, Iyama K and Baba H: Hepatobiliary and pancreatic: Large pancreatic liposarcoma. J Gastroenterol Hepatol 28: 1800, 2013.
18. Elliott TE, Albertazzi VJ and Danto LA: Pancreatic liposarcoma. Case report with review of retroperitoneal liposarcomas. Cancer 45: 1720-1723, 1980.
19. Improta L, Pasquali S, Iadecola S, Barisella M, Fiore M, Radaelli S, Colombo C, Alloni R, Callegaro D, Valeri S, *et al*: Organ infiltration and patient risk after multivisceral surgery for primary retroperitoneal liposarcomas. Ann Surg Oncol 30: 4500-4510, 2023.
20. Tyler R, Wanigasooriya K, Taniere P, Almond M, Ford S, Desai A and Beggs A: A review of retroperitoneal liposarcoma genomics. Cancer Treat Rev 86: 102013, 2020.
21. Coindre JM, Pédeutour F and Aurias A: Well-differentiated and dedifferentiated liposarcomas. Virchows Arch 456: 167-179, 2010.
22. Thway K, Flora R, Shah C, Olmos D and Fisher C: Diagnostic utility of p16, CDK4, and MDM2 as an immunohistochemical panel in distinguishing well-differentiated and dedifferentiated liposarcomas from other adipocytic tumors. Am J Surg Pathol 36: 462-469, 2012.
23. Thway K, Wang J, Swansbury J, Min T and Fisher C: Fluorescence in situ hybridization for MDM2 amplification as a routine ancillary diagnostic tool for suspected well-differentiated and dedifferentiated liposarcomas: Experience at a tertiary center. Sarcoma 2015: 1-10, 2015.
24. Sirvent N, Coindre JM, Maire G, Hostein I, Keslair F, Guillou L, Ranchere-Vince D, Terrier P and Pedeutour F: Detection of MDM2-CDK4 amplification by fluorescence in situ hybridization in 200 paraffin-embedded tumor samples: Utility in diagnosing adipocytic lesions and comparison with immunohistochemistry and real-time PCR. Am J Surg Pathol 31: 1476-1489, 2007.

25. Xu L, Xie X, Shi X, Zhang P, Liu A, Wang J and Zhang B: Potential application of genomic profiling for the diagnosis and treatment of patients with sarcoma. Oncol Lett 21: 353, 2021.
26. Win TT, Jaafar H and Yusuf Y: Relationship of angiogenic and apoptotic activities in soft-tissue sarcoma. South Asian J Cancer 3: 171-174, 2020.
27. Park BK, Koh HD, Won SY, Cho YS, Seo JH, An C and Park S: Suspicious findings observed retrospectively on CT imaging performed before the diagnosis of pancreatic cancer. J Gastrointest Oncol 14: 1008-1018, 2023.
28. He C, Zhu L, Wang X, Dai M, Wu H, Xu Q, Sun Z, Liu J, Xue H and Jin Z: Presumed radiological diagnosis of solid pseudopapillary tumors: Do we really know what we are watching? Pancreatology 23: 120-128, 2023.
29. Li DL, Li HS, Xu YK, Wang QS, Chen RY and Zhou F: Solid pseudopapillary tumor of the pancreas: Clinical features and imaging findings. Clin Imaging 48: 113-121, 2018.
30. Lo GC and Kambadakone A: MR imaging of pancreatic neuroendocrine tumors. Magn Reson Imaging Clin N Am 26: 391-403, 2018.
31. Wan Y, Hao H, Meng S, Li Z, Yu F, Chi M, Chao Q and Gao J: Application of low dose pancreas perfusion CT combined with enhancement scanning in diagnosis of pancreatic neuroendocrine tumors. Pancreatology 21: 240-245, 2021.
32. Perri G, Prakash LR and Katz MHG: Pancreatic neuroendocrine tumors. Curr Opin Gastroenterol 35: 468-477, 2019.
33. Srisajjakul S, Prapaisilp P and Bangchokdee S: CT and MR features that can help to differentiate between focal chronic pancreatitis and pancreatic cancer. Radiol Med 125: 356-364, 2020.
34. Crago AM and Dickson MA: Liposarcoma: Multimodality management and future targeted therapies. Surg Oncol Clin N Am 25: 761-773, 2016.
35. Gahvari Z and Parkes A: Dedifferentiated liposarcoma: Systemic therapy options. Curr Treat Options Oncol 21: 15, 2020.
36. Amer KM, Congiusta DV, Thomson JE, Elsamna S, Chaudhry I, Bozzo A, Amer R, Siracuse B, Ghert M and Beebe KS: Epidemiology and survival of liposarcoma and its subtypes: A dual database analysis. J Clin Orthop Trauma 11: S479-S484, 2020.